Effects of Parkinson's Disease-Linked Mutations on the Structure of Lipid-Associated α-Synuclein†

Robert Bussell Jr.‡ and David Eliezer*,§

Department of Physiology, Biophysics and Molecular Medicine and Department of Biochemistry and Program in Structural Biology, Weill Medical College of Cornell University, 1300 York Avenue, New York, New York 10021

Received November 26, 2003; Revised Manuscript Received February 17, 2004

ABSTRACT: α-Synuclein (αS) is a lipid-binding synaptic protein of unknown function that is found in an aggregated amyloid fibril form in the intraneuronal Lewy body deposits that are a defining characteristic of Parkinson's disease (PD). Although intrinsically unstructured when free in solution, αS adopts a highly helical conformation in association with lipid membranes or membrane mimetic detergent micelles. Two mutations in the αS gene have been linked to early onset autosomal dominant hereditary forms of PD, and have been shown to affect the aggregation kinetics of the protein in vitro. We have used high-resolution NMR spectroscopy, circular dichroism, and limited proteolysis to investigate the effects of these PD-linked mutations on the helical structure adopted by αS in the lipid or detergent micelle-bound form. We show that neither the A53T nor the A30P mutation has a significant effect on the structure of the folded protein, although the A30P mutation may cause a minor perturbation in the helical structure around the site of the mutation. The A30P, but not the A53T, mutation also appears to decrease the affinity of the protein for lipid surfaces, possibly by perturbing the nascent helical structure of the free protein. The potential implications of these results for the role of αS in PD are discussed.

The importance of α-synuclein (αS)[1] in the pathogenesis of Parkinson's disease (PD) was first established by the discovery of two mutations in the αS gene that segregate with early onset hereditary forms of PD (*1*, *2*). This was followed by the discovery that αS is a major component of the spherical intraneuronal proteinaceous Lewy body deposits that are a hallmark of PD (*3*). The observation that αS is found in Lewy bodies in an aggregated amyloid fibril form suggested that αS aggregation was important in the development of PD. Some support for this hypothesis is provided by the observation that the early onset PD mutations are associated with more rapid αS oligomerization in vitro (*4*−*6*), observations that αS oligomers are capable of permeabilizing lipid bilayers (*7*), and a report that αS can form covalent adducts with dopamine which accumulate in an oligomeric state (*8*). Additional evidence linking αS to PD is provided by transgenic flies and mice expressing human αS, which have been shown to exhibit PD-like disorders (*9*, *10*).

The normal function of αS remains poorly understood, but is believed to involve an interaction with synaptic vesicles, which is likely to be transient and/or reversible (*11*). Such reversible lipid membrane binding is suggested by the sequence of the protein, which includes a number of imperfect 11-mer tandem repeats that are reminiscent in character of those observed in apolipoprotein sequences (*12*, *13*). The purpose of lipid or vesicle binding by αS is unclear. On the basis of our observations that the C-terminal tail of αS does not interact with lipid vesicles or lipid mimetic detergent micelles, we have proposed that αS may anchor synaptic vesicles to cytoskeletal components through interactions with its C-terminus (*14*). A number of cytoskeletal proteins have been reported to interact with αS, including tau (*15*) and tubulin (*16*), and in the case of tau, the interaction site was reported to be in the C-terminal region of αS. Another potential function for αS is regulation of the enzyme phospholipase D2 (PLD2), which converts phosphatidylcholine to phosphatidic acid, which is in turn a regulator of synaptic vesicle formation (*17*). αS interactions with phosphatidic acid containing membranes (*18*) may modulate PLD2 regulation resulting in a feedback loop (*19*). Studies of mice lacking αS have suggested a role for αS in the regulation of synaptic vesicle recycling or pool size (*20*−*22*). Recently, reported interactions between αS and the human dopamine transporter (hDAT) have suggested a role for αS in the regulation of dopamine uptake into synaptic vesicles (*23*, *24*).

The effects of the two PD-linked mutations A30P and A53T on the lipid interactions of αS have been investigated by a number of groups with somewhat conflicting results. The A53T mutation appears to have little effect on αS lipid interactions, but several reports indicate that the A30P mutation decreases the extent of αS membrane binding in vitro (*25*, *26*) and in vivo (*27*, *28*). Such an effect could directly influence the normal function of the protein, but

† This work was supported in part by the NIA, National Institutes of Health, Grant AG19391 (to D.E.) and by a gift from Herbert and Ann Siegel (to D.E.).

* To whom correspondence should be addressed. E-mail: dae2005@med.cornell.edu, 212-746-6557 (tel) or 212-746-4843 (fax).

‡ Department of Physiology, Biophysics and Molecular Medicine.

§ Department of Biochemistry and Program in Structural Biology.

[1] Abbreviations: αS, α-synuclein; PD, Parkinson's disease; CD, circular dichroism; POPC, 1-palmitoyl 2-oleoyl phosphatidylcholine; POPA, 1-palmitoyl 2-oleoyl phosphatidic acid; POPS, 1-palmitoyl 2-oleoyl phosphatidylserine; PLD2, phospholipase D2; hDAT, human dopamine transporter; APP, amyloid-β precursor protein.

10.1021/bi036135+ CCC: $27.50
Published on Web 03/27/2004

could also enhance aggregation by increasing the concentration of the aggregation prone free state, as we suggested based on our studies of the free state of the A30P mutant (*29*).

Previously, we have characterized the structure of wild-type αS bound to lipid-mimetic detergent micelles and determined that the protein adopts two long stretches of helical structure (*30*). Here, we investigate the effects of the two PD-linked mutations, A30P and A53T, on the micelle-bound and lipid vesicle bound conformation of the protein to assess the potential effects of these mutations on its normal function and to evaluate any implications these effects may have for the role of αS in PD. We find that both αS mutants are nearly identical to the wild-type protein in their detergent micelle and lipid-bound structure. The A30P mutant, however, exhibits a somewhat decreased affinity for lipid surfaces, possibly as a consequence of the perturbation in the nascent helical structure of the free protein that we previously documented for this mutant (*29*).

METHODS

Recombinant wild type, A30P, and A53T αS were produced and purified as previously described (*14*, *29*). Because we previously determined that the C-terminal ~40 residues of αS do not interact with lipid vesicles or detergent micelles (*14*), we also constructed truncated variants of wild type and mutant αS proteins by using site-directed mutagenesis to place a stop codon at the position corresponding to residue 103 in our expression constructs. The correct truncated wild type and mutant sequences were verified by sequencing the modified constructs. The truncated proteins were produced and purified in the same manner as the wild-type protein, except that truncation abrogated retention of the proteins during anion exchange chromatography, which actually facilitated the purification process as most other proteins in the bacterial cell lysates were retained on the column. The composition and purity of all protein constructs were verified using mass spectrometry, SDS−PAGE, and NMR. NMR samples of micelle-bound αS were produced in 100 mM NaCl, 10 mM Na_2HPO_4, 40 mM ^{2}H-SDS, pH 7.4 in 90%/10% H_2O/D_2O as previously described for the wild-type protein (*14*), using both full-length and truncated constructs, and contained approximately 7 mg/mL of protein. NMR spectra of micelle containing samples were collected at 40 °C on a 600 MHz Varian Unity INOVA spectrometer using modern versions of standard pulse sequences. NMR data acquisition and data processing parameters were as reported previously (*30*). Truncation of the protein resulted in the absence of resonances from the C-terminal tail, leading to less congested spectra with improved signal-to-noise. Resonances were assigned based on HNCACB/CBCACONH and HNCACO/HNCO pairs of triple resonance experiments collected for both the full-length and truncated versions of the A30P and A53T mutants, as well as for the truncated wild-type protein (the full-length wild-type protein having been previously assigned (*30*)). Sequential amide proton NOEs were obtained from HSQC−NOESY−HSQC spectra collected with a 300-ms mixing time using fractionally deuterated protein. NOESY spectra were collected with truncated variants to eliminate spectral overlap with resonances from the C-terminal tail region.

Small unilamellar lipid vesicles were prepared in 100 mM NaCl, 10 mM Na_2HPO_4, pH 7.4 using a sonication method as previously described (*14*). NMR samples of lipid vesicle bound αS were prepared as previously described (*14*) by mixing solutions of the free protein with lipid vesicle preparations. Final protein concentrations were approximately 1 mg/mL. NMR spectra of lipid vesicle containing samples were collected at 10 °C.

Limited proteolysis was performed at 24 °C using full-length wild type and mutant protein samples prepared in the same manner as the NMR samples with final protein concentrations of approximately 1 mg/mL. Digestions in the presence of both SDS detergent micelles and lipid vesicles employed the relatively nonspecific protease subtilisin, as described previously (*30*), except that for digests performed in the presence of lipid vesicles, either a C18 bead based or a chloroform-based extraction was used prior to gel electrophoresis. This was done to remove lipids from the sample and prevent lipid-associated degradation of the SDS−PAGE results (see below). For the C18 bead extraction digested protein samples were bound in batch mode to C18 beads preequilibrated with 0.1% TFA in water, washed with 0.1% TFA in water, eluted with 90% acetonitrile, 0.1% TFA in water, dried on a Speed-Vap, and resuspended in phosphate buffered saline prior to SDS−PAGE. For the chloroform extraction aliquots of digested protein samples were added to a chloroform/methanol mixture in an 8:4:1 ratio, vortexed, and centrifuged. The denser organic phase was aspirated away and the aqueous phase was lyophylized, leaving the protein-containing interface region, which was resuspended in phosphate buffered saline prior to SDS−PAGE. Several lipid vesicle compositions were used, including 50%/50% POPA/POPC, 30%/70% POPS/POPC (using either synthetic or brain derived POPS), 100% POPC, or 100% POPA.

Circular dichroism (CD) data were collected at 24 °C on an AVIV 62 DS spectrometer equipped with a sample temperature controller using a 0.2-mm path length cell under buffer conditions identical to those used in the NMR experiments, at protein concentrations of 1 mg/mL. Protein concentrations were also measured using absorption at 280 nm.

RESULTS

Structure of Micelle Bound αS Is Largely Unaffected by A30P and A53T Mutations. To facilitate our NMR studies of detergent micelle-bound αS mutants, we truncated the wild type and mutant proteins after position 102, since our previous results indicated that residues beyond this position did not interact with micelles (*14*, *30*). As expected, removal of the C-terminal tail resulted in better resolved NMR spectra of micelle-bound αS that could be assigned in a straightforward fashion using triple resonance methods. The assigned proton−nitrogen correlation spectrum of the wild-type protein is shown in Figure 1. The deviation of the Cα chemical shift from random coil values is a useful indicator of secondary structure propensities at local sites in proteins, with positive values indicative of helical structure, and negative values indicative of extended or strand like structure. When plotted as a function of residue number the Cα chemical shift data from truncated wild-type αS (Figure 2a) are nearly identical to those obtained previously for the full-

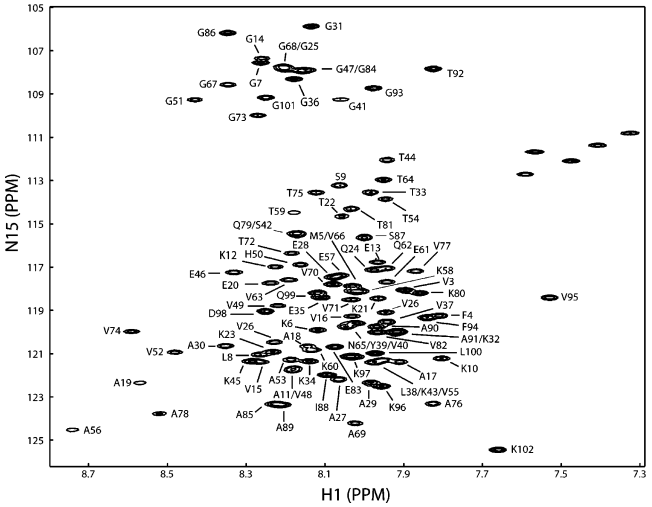

FIGURE 1: The proton nitrogen correlation spectrum (HSQC) of SDS micelle-bound wild-type truncated αS. Backbone resonance assignments are indicated. Unlabeled peaks at the right correspond to side chain amides.

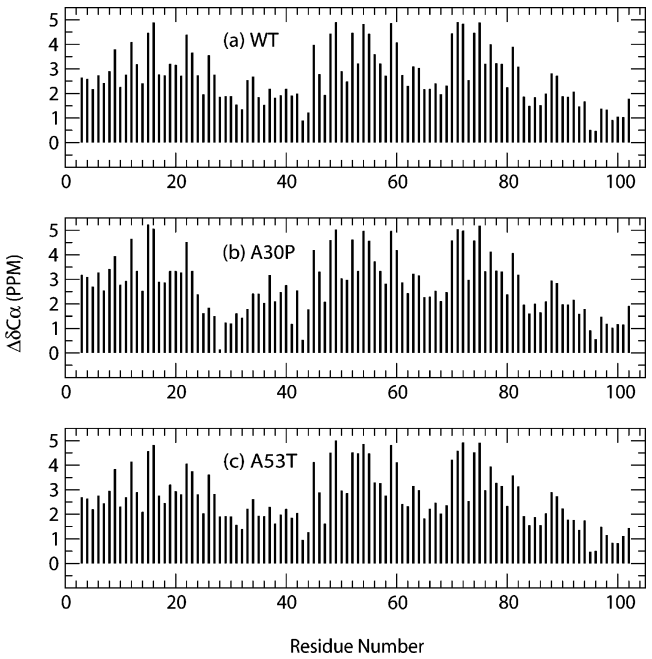

FIGURE 2: Cα secondary shifts (the deviation of the Cα chemical shift from the value expected in a random coil conformation) for truncated SDS micelle-bound wild type (a), A30P (b), and A53T (c) αS. These shifts are strongly correlated to the backbone dihedral ϕ,ψ angles (*43*, *44*) with positive values indicating helical structure and negative values indicating extended or strand-like structure. Errors are estimated at less than 0.2 ppm.

length protein (*30*), demonstrating that the truncation of the C-terminal tail does not affect the structure of the micelle-bound conformation. When compared with the data for the wild-type protein, the Cα shift deviations for each of the two early onset PD-linked mutants of αS (Figure 2) reveal that the mutations have a minimal effect on the structure of the micelle-bound state of the protein, with both mutants displaying the small Cα shift deviations at position 43 that were previously observed in the wild-type protein. In the A30P data, it appears that the mutation may slightly destabilize or alter the protein's helical structure locally around the site of the mutation, as reflected by the greatly reduced Cα shift deviation of Glu 28. The A53T data are

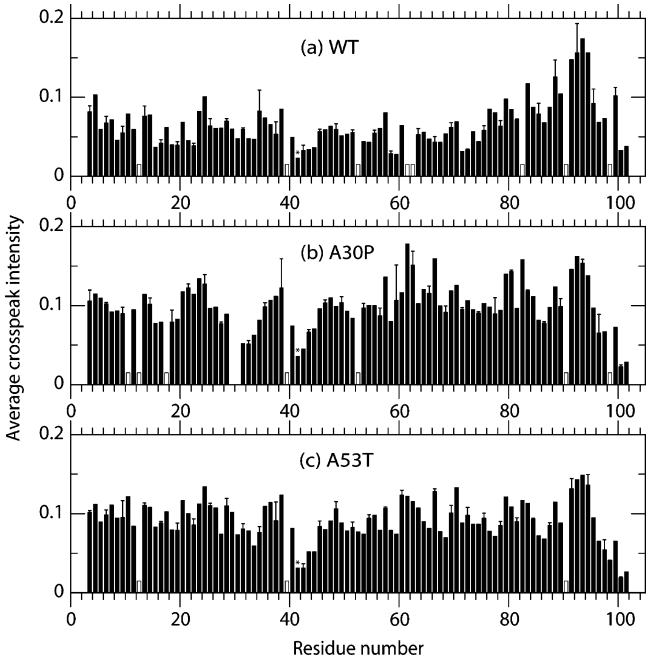

FIGURE 3: Sequential amide proton to amide proton NOEs in truncated SDS micelle-bound wild type (a), A30P (b), and A53T (c) αS. Strong NOEs are associated with short NH−NH distances such as those present in helical structure. Intensities represent the average of the two symmetric NOE peaks. The asterisk-marked bar between positions 41 and 42 represents only the intensity of the NOE from residue 41 to 42 because no NOE was observed from residue 42 to 41. Short unfilled bars represent resonance overlap between neighboring residues, precluding a determination of the presence of absence of these sequential NOEs. No NOEs are possible to or from position 30 in the A30P data because proline lacks an amide proton. Error estimates are shown every third data point.

nearly identical to those from the wild-type protein, indicating that this mutation has no detectable effect on the structure of micelle-bound αS. To confirm that truncation of the mutant proteins did not introduce any artifacts, we also assigned the backbone resonances of full-length A30P and A53T αS. The Cα shift data from the full-length mutants (not shown) are essentially identical to those of the truncated versions, and also show no significant differences between the wild type and mutant proteins in the C-terminal tail region.

These observations are complemented by measurements of sequential amide proton to amide proton NOEs. This NOE parameter is a measure of the physical distance between successive amide protons in the protein, and is expected to have a relatively large value for helical structure (where this distance is short) and a much smaller value for extended or strand-like structure (where this distance is large). The NOE data for both the A30P and A53T truncated mutants are essentially indistinguishable from those observed for wild-type αS (Figure 3), both at and away from mutation sites, indicating that neither mutation significantly perturbs the local geometry of the micelle-bound protein. The improved signal-to-noise ratio in the data from the truncated proteins allowed for detection of weak previously unobserved NOE signals from residues 41 to 42 and 42 to 43. We note that NOE cross-peak intensity can be affected by the intensity of the corresponding diagonal resonances (*31*), which in turn can be attenuated by other relaxation processes. Therefore, it is possible that residue 42 may be undergoing unusual

dynamics that contribute to the weak NOE signals observed for this residue. Slightly different dynamics may also account for the increased NOE intensities near the C-terminal end of the truncated proteins.

To further probe the effects of the two PD-linked mutations on the structure of both micelle and lipid vesicle bound αS, we employed limited proteolysis using the relatively non-specific protease subtilisin. We previously demonstrated that in the micelle-bound state of the full-length wild-type protein, residues 1−103 form a stable intermediate during subtilisin digestion, being protected from initial cleavage relative to more C-terminal residues and remaining observable using SDS−PAGE after the full-length protein band has entirely disappeared (*30*). The kinetics of proteolysis of the SDS micelle-bound full-length protein are essentially unchanged in either of the two mutants (see Supporting Information), which are both protected in the same manner. This suggests that both mutants bind to SDS micelles in a fashion similar to that of the wild-type protein, and that neither mutation significantly decreases the affinity of the protein for detergent micelles, as such a perturbation would be expected to lead to more rapid proteolysis of the protein.

In the Presence of Lipid Vesicles a Subpopulation of αS Remains Lipid Free. In our studies of the wild-type protein (*30*), we reported that the lipid vesicle bound state of αS is degraded in a two-state transition (from full-length protein to small peptides without intermediate products) and must therefore be in rapid equilibrium with a minor population of free protein which is unprotected from proteolytic degradation. Our current results support this conclusion and indicate that it applies to both αS mutants as well, and holds equally for all lipid vesicle compositions tested except for 100% POPC, which is bound only weakly by αS. In particular, we are now able to detect and identify some of the protein fragments that are produced in digestions of the vesicle-bound protein. The presence of lipids interferes with SDS−PAGE of digestion reactions and prevented us from previously observing intermediate degradation products during digestion of the lipid vesicle bound protein (*30*). A recent study of synuclein aggregation also reports that lipids interfere with SDS−PAGE detection of this protein (*32*). In the current experiments, we removed lipids from vesicle containing digests prior to SDS−PAGE and were then able to observe proteolytic products. Consistent with our previous report (*30*), the digestion pattern of vesicle-bound wild-type (and mutant) αS is clearly different from that of the micelle-bound protein. Specifically, no prominent band corresponding to residues 1−103 is observed for any of the three αS variants in the vesicle-bound state digestions. Instead, four primary cleavage products appear almost simultaneously, two migrating more slowly and two more quickly than the 1−103 fragment (Figure 4).

N-terminal sequencing indicates that all four bands that appear initially in digests of vesicle-bound wild-type αS contain the N-terminus of the intact protein. The two upper bands migrate identically to bands observed in the cleavage reaction of the micelle-bound protein (Figure 4) that were previously identified as αS fragments 1−113 and 1−125 (*30*), and the presence of the N-terminus of the intact protein in these bands suggests that these same fragments are produced in the presence of lipid vesicles. Each of the two upper bands also contains an N-terminus corresponding to

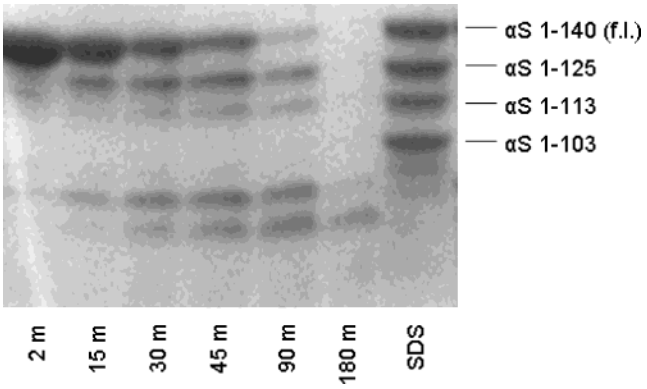

FIGURE 4: SDS−PAGE monitored proteolytic digestion of POPA/POPC bound wild type αS at a protease to protein mass ratio of 1:1000 at different time points, as indicated. The last lane represents a digestion in the presence of SDS micelles, and the previously determined identities of the αS fragments are indicated to provide a reference.

Glu 57 and Gly 73, respectively. Cleavage at these locations is confirmed by the detection of peptide masses corresponding to fragments 1−56 (5663), 1−72 (7305), 57−140 (8816), and 73−140 (7174) in electrospray mass spectra of digestion reactions in the presence of lipid vesicles (not shown). This suggests that the bottom two bands are fragments 1−56 and 1−72 and that the top two bands contain fragments 57−140 and 73−140, respectively, in addition to the previously mentioned fragments. The two latter fragments migrate more slowly than predicted based solely on their masses, but this behavior is typical of proteolytic and recombinant fragments of αS that contain the highly acidic C-terminal region.

In our earlier work (*14*), we showed that the N-terminal ~100 residues of wild-type αS bind to POPA/POPC lipid vesicles. Although we cannot directly observe the conformation of these lipid-bound residues using NMR (lipid associated residues tumble at the same slow rate as the lipid vesicle, leading to undetectably broad NMR lines), CD spectra clearly demonstrated that they adopt a helical conformation, and together these observations indicated that the conformation of the lipid-bound protein closely resembles that of the micelle-bound protein. Therefore, we do not expect the lipid-bound region of the protein to be susceptible to proteolysis at the observed cleavage sites. Rather, the present observation of αS cleavage after positions 56 and 72 suggests, in agreement with our original conclusion (*30*), that in the presence of phospholipid vesicles, αS exists in an equilibrium between the lipid-bound and the lipid-free state, and that proteolysis occurs predominantly in the minor population of the intrinsically unstructured free state. In this case, the specific cleavage products we observe are related to the intrinsic preference of the protease, and not to structural properties of the lipid-bound protein.

In support of this hypothesis, we previously reported that NMR proton−nitrogen correlation spectra of POPA/POPC vesicle containing αS samples reveal, in addition to strong signals from the unstructured C-terminal tail, a weak background containing the complete spectrum of the free protein, indicating a minor population of lipid free αS. We have now repeated this observation for αS in the presence of pure POPA, POPA/POPC, and of POPS/POPC vesicles with similar results (Figure 5a−c). In contrast, in the presence of pure POPC vesicles, we observe all the resonances from

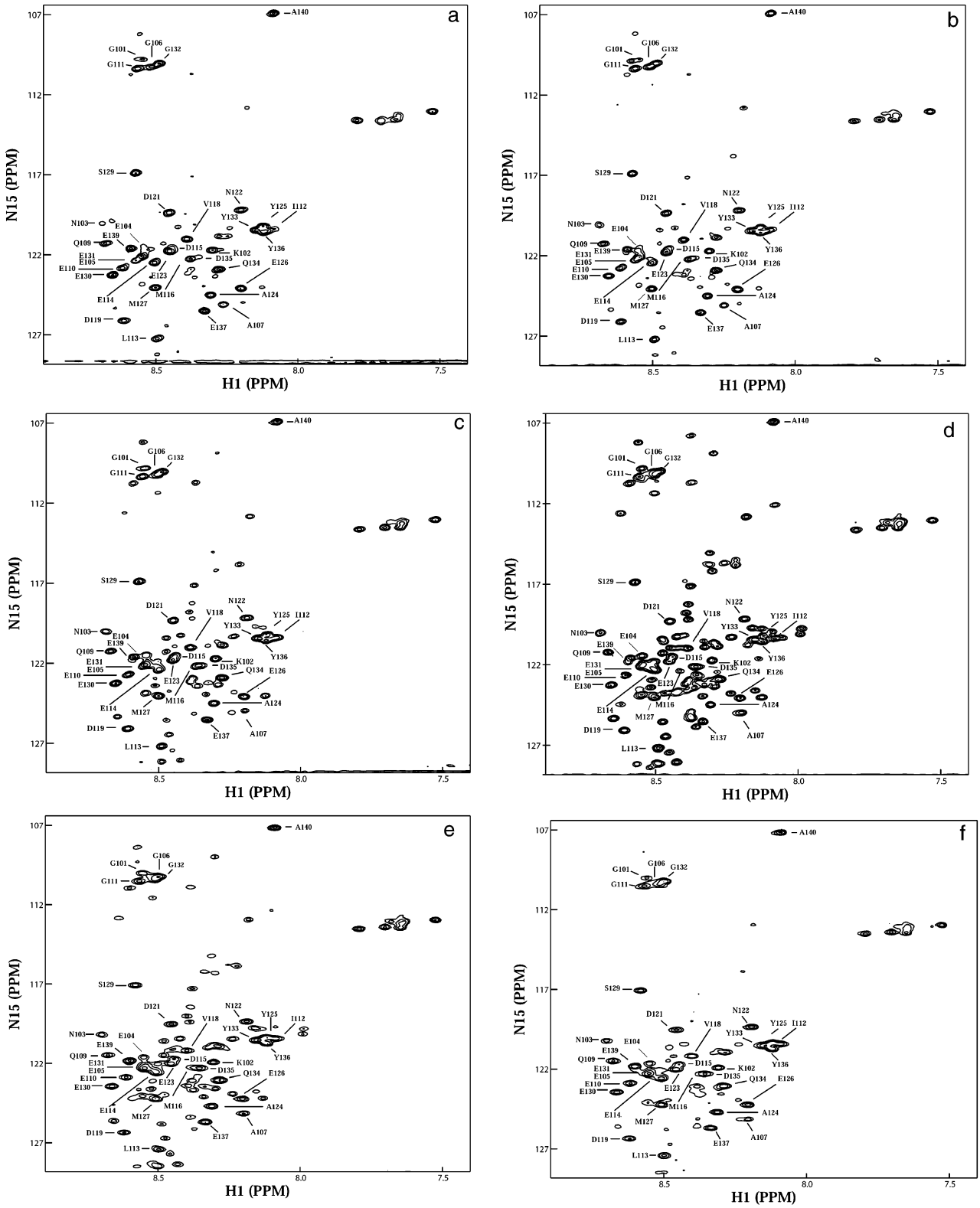

FIGURE 5: Proton−nitrogen correlation spectra for wild-type αS in the presence of (a) POPA, (b) POPS/POPC, (c) POPA/POPC, (d) POPC lipid vesicles and for (e) A30P and (f) A53T αS in the presence of POPA/POPC lipid vesicles. Strong resonances are observed from the C-terminal tail of both lipid-bound and lipid-free protein and are individually labeled. Resonances originating from the N-terminus arise only from lipid-free protein. All spectra were collected at equal protein concentrations, processed identically, and plotted at identical contour levels.

the spectrum of the free protein at significant intensity (Figure 5d), indicating a relatively weak interaction between αS and POPC vesicles and a larger fraction of lipid free protein. This is consistent with the observation of more rapid degradation of αS in the presence of POPC vesicles compared to POPA, POPA/POPC, or POPS/POPC.

The Equilibrium between Lipid Bound and Lipid Free αS Is Sensitive to Lipid Composition. We attempted to quantitate

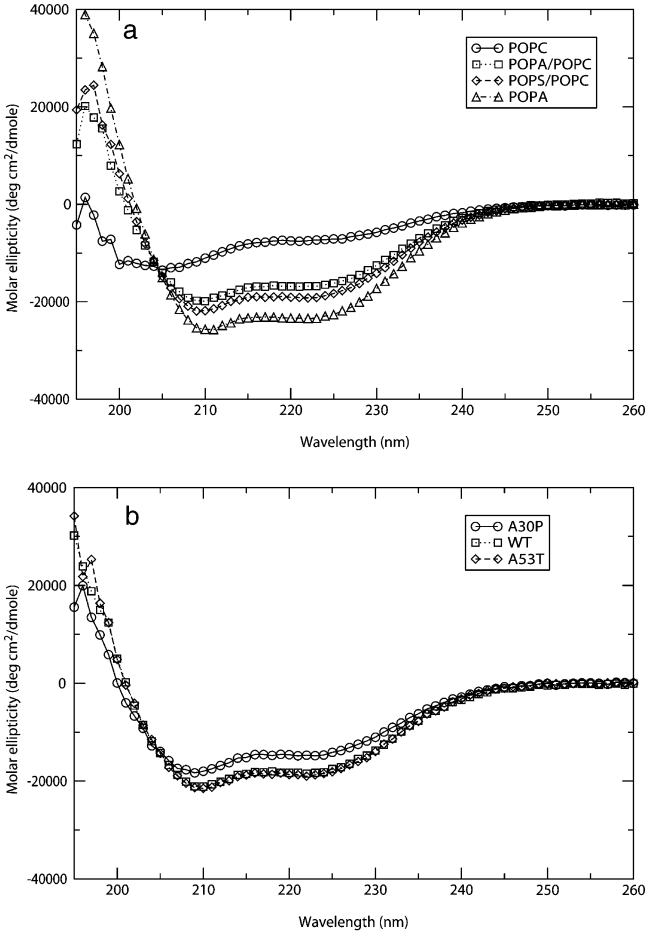

FIGURE 6: CD data from (a) wild-type αS in the presence of POPA, POPS/POPC, POPA/POPC, and POPC vesicles and (b) wild type, A30P, and A53T αS in the presence of POPA/POPC vesicles.

the fraction of αS that is lipid-free in the presence of each type of lipid vesicle by comparing the intensities of resonances from the lipid associated N-terminal region (which originate only from free protein) with those of peaks from the lipid free C-terminal tail (which originate from both free and lipid-bound protein). We integrated peak intensities from positions 1−102 and normalized them by the integrated peak intensities from positions 118−140. Using this method, we estimate that the fraction of αS in the lipid-free state is around 8 ± 1%, 16 ± 2%, 24 ± 2%, and 61 ± 3% for POPA, POPS/POPC, POPA/POPC, and POPC vesicles, respectively.

CD spectra from wild-type αS in the presence of POPA, POPS/POPC, and POPA/POPC vesicles confirmed that the bulk of the protein is lipid associated, and that the lipid associated conformation is highly helical (Figure 6a). The CD signal at 222 nm, which is sensitive to helical structure content was strongest for POPA vesicles and somewhat weaker for POPS/POPC and POPA/POPC vesicles. In the presence of POPC vesicles, CD spectra indicated a much lower degree of helical structure content, suggesting that much less of the protein is lipid associated. Helical content as judged by CD was observed to depend on both protein and lipid concentration (data not shown), consistent with an appreciable and fluctuating equilibrium population of lipid-free protein (see Supporting Information). The CD results, like those from the NMR proton−nitrogen correlation spectra, also indicate that the interactions of αS with lipid vesicles are sensitive to lipid composition.

A30P, but not A53T, Decreases the Affinity of αS for Lipid Vesicles. The kinetics of αS digestion in the lipid vesicle bound state (Figure 4 and data not shown) were found to be relatively insensitive to the presence of either PD-associated mutation. CD spectra (Figure 6b) and NMR proton−nitrogen correlation spectra (Figure 5e−f) confirm that the interactions of the two PD-linked mutants with POPA/POPC lipid vesicles are very similar to those of the wild type, with both mutants possessing a highly helical structure as indicated by the CD data, having free C-terminal tails and lipid associated N-terminal regions as indicated by the NMR spectra, and showing a minor population of lipid-free protein, as also shown by the NMR spectra. The A30P mutant, however, clearly exhibits a higher population of lipid-free protein, as indicated by relatively higher intensities of lipid-free NMR resonances from the N-terminal lipid binding region (Figure 5e) and a lower helical content indicated by CD spectra of this mutant (Figure 6b). Using the methods described above, we quantitated the lipid-free fractions of A53T and A30P αS in the presence of POPA/POPC and compared the results to those obtained for the wild-type protein. Wild type and A53T αS exhibited similar lipid-free populations of around 14 ± 2% and 20 ± 2%, respectively, as determined from NMR spectra. In contrast, A30P showed a significantly greater lipid-free population, estimated at 36 ± 3%.

DISCUSSION

Aggregation and amyloid fibril formation are thought to be intimately linked to the role of αS in the pathogenesis of PD and to the role of other amyloidogenic proteins in the respective diseases with which they are associated. Nevertheless, in several cases including αS, APP, and tau arguments remain that some aspects of the normal function of these proteins may contribute to their involvement in neurodegeneration. In the case of αS, this normal function involves lipid interactions, including an association with synaptic vesicles (*11*). Perturbation of the interactions of αS with synaptic vesicles and of its purported role in synaptic vesicle production or regulation could potentially play a role in the disruption of dopamine production and release that is a key feature of PD. Interference with the interactions of αS with lipids could also play a role in αS aggregation. Increasing the cytosolic concentration of αS could increase the in vivo aggregation rate of the free protein (which has been shown to aggregate and form amyloid fibrils in vitro). In addition, disturbing the structure of lipid-bound αS could enhance any aggregation process that involves the membrane-bound state of the protein (αS aggregation has also been reported to occur on lipid surfaces (*27*, *33*)).

Two mutations in the gene coding for αS, A30P and A53T, have been linked to familial forms of early onset PD (*1*, *2*). A number of studies have shown that both of these mutations enhance the rate of oligomerization of the free protein (*4*, *5*, *34*, *35*), although the A30P mutation retards mature fibril formation, while the A53T mutation leads to faster mature fibril formation (*6*). These observations contributed to a model in which αS toxicity in PD is mediated by oligomeric species of the protein, which may interact with and possibly permeabilize cellular membranes (*36*). In this model, the enhanced toxicity of the PD-linked αS mutants is explained by their propensity to form oligomers more rapidly than the

wild-type protein. Another mechanism by which mutations could conceivably increase αS toxicity is by interfering with the normal interactions of monomeric αS with lipids and thereby perturbing its function. The effects of the two mutations on αS lipid interactions have been investigated in vivo and in vitro. The A53T mutation appears to have little effect on αS lipid binding, while for A30P more variable results have been described. Jo et al. reported that the A30P mutant is defective in binding phospholipid vesicles in vitro (*26*). Jensen et al. reported that the A30P, but not the A53T mutation disrupts interactions formed by the wild-type protein with vesicles isolated from rat brain (*28*). Perrin et al. reported that A30P αS interacts with POPA/POPC phospholipid vesicles nearly to the degree that the wild-type protein does, but shows weaker interactions and less helical structure in the presence of POPS/POPC vesicles (*25*). They observed no difference between the interactions of A53T and wild-type αS with either type of phospholipid vesicle. Cole et al. observed that A30P did not bind to lipid droplets after loading cells with fatty acids, while wild type and A53T αS relocated from the cytoplasm to lipid droplet surfaces (*27*). McLean et al. observed no effect of either PD mutation on the interactions of αS with membranes in intact neurons (*37*), although they did observe evidence for an altered conformation in the case of A30P. Kahle et al. observed similar synaptosomal localization, presynaptic destribution and anterograde transport of wild type and A30P αS in transgenic mice (*38*).

Despite the likely involvement of αS aggregation in the pathogenesis of PD, it remains possible that some disruption or modification of the normal function of αS plays a role in the onset or progression of this disease. This possibility is accentuated by the fact that various clues regarding the normal role of αS in neurons suggest a function involving the regulation of dopamine containing synaptic vesicles, when considered in light of the fact that PD is fundamentally a syndrome of dopamine deficiency. The evidence for αS involvement in dopamine vesicle regulation includes the observations that αS interacts (probably reversibly) with synaptic vesicles (*19*, *37*, *38*), that αS may regulate synaptic vesicle biogenesis through interactions with PLD2 (*17*), and that αS regulates the human dopamine transporter hDAT (*23*, *24*). In each of these cases, the relevant functional form of αS is very likely the lipid-bound state. Therefore, any potential PD-related modification of the normal function of αS by PD-linked mutations is likely to be mediated by changes in αS lipid interactions.

In our previous study of the two PD-linked mutants of αS, we used high resolution solution NMR spectroscopy to characterize the effects of the mutations on the structural properties of the predominantly unstructured free protein, and discovered that the A30P mutation disrupted a stretch of residual helical structure (*29*). In this work, we have used NMR combined with CD and limited proteolysis to compare the structural properties of the two PD-linked αS mutants with those previously observed in our studies of the wild-type protein in association with lipid mimetic detergent micelles and phospholipid vesicles (*30*). By analyzing NMR Cα chemical shifts and sequential amide proton NOEs, we show that the A53T mutation has no detectable effect on the structure of the micelle-bound protein, and the A30P mutation has only a minor effect. Both mutants, like the wild type, exhibit a highly helical structure as indicated by large positive Cα chemical shift deviations (Figure 2), strong sequential amide proton NOEs (Figure 3) and CD data (Figure 6). Both mutants, like the wild type, show only a single potential interruption in this helical structure at positions 42−43 as indicated by small Cα chemical shift deviations and weak or absent sequential amide proton NOE signals. The A30P mutant also shows a greatly reduced Cα shift for residue 28, but no interruption is observed in the NOE data around this location (the absence of NOEs at position 30 results from the lack of an amide proton in proline), suggesting that any perturbation of the helical structure at this location must be small. In agreement with this result, we find that all three αS variants (wild type and the two mutants) are similarly susceptible to proteolytic degradation in association with detergent micelles (see Supporting Information), being proteolyzed with similar time constants and producing the same proteolytic fragments. This suggests that similar structural features protect all three micelle-bound variants from proteolysis and that the affinities of each variant for detergent micelles must be similarly high.

It is perhaps not surprising that the A53T mutation in αS does not dramatically perturb the micelle-stabilized helical structure of the protein because, although threonine is more commonly found in β-sheet structure than in α-helical structure (*39*), it is not generally considered a helix-breaking residue. More surprising, however, is the apparent ability of the helical structure of the micelle-bound protein to tolerate the substitution of a proline for an alanine at position 30. Prolines are generally considered helix-breaking residues (*39*), and are not favored in the middle of helices. Nevertheless, prolines can occur within helices, and when they do they typically lead to kinks, rather than breaks, in the helical structure. A typical example is the presence of a proline residue in the middle of the F helix of sperm whale myoglobin. Another example is the presence of numerous prolines in an all helical structure of apolipoprotein A-I (*40*), a protein with structural and functional similarities to αS. In both these cases, the prolines are associated with kinks in helices. Also in both cases, the kinked helical structure is thought to be stabilized by strong hydrophobic interactions, with the heme group in the case of myoglobin (*41*), and with lipids in the case of apoAI (*42*). It is possible that the A30P mutation in αS also leads to a kink in the first of the two helices in the structure of micelle-bound αS, and this might be reflected in the anomalous Cα shift deviation of Glu 28.

We are not able to directly observe the structure of lipid-bound αS using NMR. Therefore, we resorted to other methods to characterize the lipid-bound protein and to compare it with our observations of the micelle-bound state. Our results show that αS interacts more weakly with lipid vesicles than with SDS detergent micelles. While digestion in the presence of SDS micelles reveals significant protection of the micelle-bound region of the protein from proteolysis, degradation of αS in the presence of lipid vesicles (Figures 4 and 7) takes place predominantly via the free state, suggesting that a small population of protease-accessible lipid-free protein is in equilibrium with the lipid vesicle bound state. This is confirmed by clear evidence for lipid-free protein in NMR spectra of αS in the presence of lipid vesicles. The fraction of lipid-free αS determined from the NMR data depends on the lipid vesicle composition, with

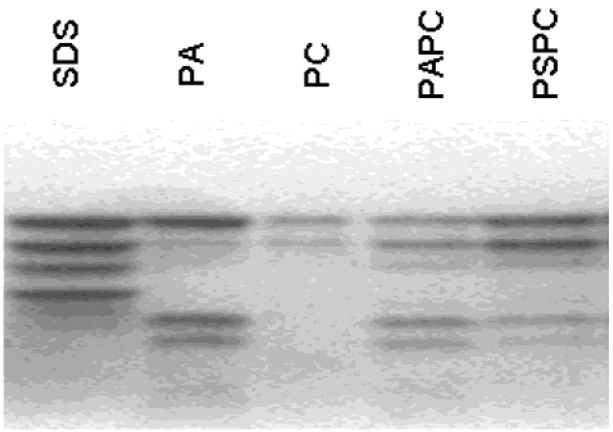

FIGURE 7: SDS−PAGE monitored proteolytic digestion of wild-type αS after 45 min at a protease to protein mass ratio of 1:1000 in the presence of POPA, POPC, POPA/POPC, and POPS/POPC lipid vesicles. A digestion in the presence of SDS micelles is provided for a reference.

pure POPA vesicles showing the lowest population of free protein, POPS/POPC and POPA/POPC showing slightly increasing levels of free protein, and POPC showing a significantly larger fraction of unbound protein. Since the equilibrium between vesicle-free and vesicle-bound protein (at a given protein and lipid concentration) is determined by the protein-to-vesicle binding constant, we conclude that the affinity of αS for lipid vesicles is dependent on vesicle composition, but is relatively low for any of the examined vesicles, since an observable population of vesicle-free protein exists even with pure POPA vesicles. Of the compositions used here, pure POPA vesicles have the highest affinity for αS, but this affinity is still less than that of the protein for SDS micelles, in the presence of which no free protein is observed by NMR or limited proteolysis. This result suggests that surface negative charge distribution is a crucial determinant of αS lipid interactions, with a denser charge, such as might be expected on an SDS micelle surface, leading to higher binding affinity. On the basis of this observation, we propose that in vivo, the localization of αS may be regulated by the lipid composition of its target membranes, and that the protein's function may involve the sensing of membrane lipid composition, perhaps in the context of synaptic vesicle biogenesis.

Our observations of A30P and A53T αS lipid vesicle interactions revealed that the A53T mutation does not significantly perturb the binding of the protein to lipid vesicles, as judged by the population of free protein in the presence of lipid vesicles. In contrast, the A30P mutation results in a significantly increased population of lipid-free protein, indicating that this mutation decreases the affinity of αS for lipid surfaces. This result is in accord with several previous in vitro and in vivo studies of αS lipid interactions (*25*−*28*). The mechanism by which this mutation exerts this effect is not clear at this time. On the basis of our direct observation and comparison of the structural properties of the wild type and A30P proteins bound to detergent micelles, we expect that the lipid-bound structure of the A30P mutant will be quite similar to that of the wild-type protein, with only a small perturbation, such as a kink in the helical structure near the site of mutation. Nevertheless, even such a small perturbation may reduce the strength of the interaction between the protein and the lipid surface, resulting in the observed decrease in binding affinity. A second possibility is suggested by our earlier studies of lipid-free αS (*29*), in which we observed that the A30P mutation disrupts a region of nascent or residual helical structure that we proposed might form an initiation site for the folding of the protein into the lipid-bound conformation. We proposed that this structural perturbation could retard αS folding and either concomitant or subsequent lipid association, resulting in a decreased affinity of the mutant protein for lipid surfaces. These two possible explanations for the reduced affinity of A30P αS for lipid vesicles are not mutually exclusive, and further studies will be required to determine which, if either, is correct.

CONCLUSIONS

The affinity of αS for lipid surfaces is sensitive to lipid composition, and the protein's function may involve sensing the lipid composition of its target membrane. The lipid interactions and lipid-induced structures of wild-type αS and its PD-linked mutant A53T are nearly identical to each other. In contrast, the A30P mutation decreases the affinity of αS for lipid surfaces and results in a small perturbation of the lipid-bound conformation of the protein. Aggregation of A30P αS may be enhanced either by the increased population of lipid-free protein expected to result from the decreased lipid affinity of this mutant, or through an aggregation pathway directly involving the structurally perturbed lipid-bound form of the mutant protein. In addition, however, the described effects of the A30P mutation may alter or interfere with the normal function of the protein in a manner that may contribute to the role of this αS mutation in PD.

ACKNOWLEDGMENT

We thank Dr. Peter Lansbury (Harvard Medical School) for valuable discussions and for generously providing us with the α-synuclein gene constructs. We are also grateful to Gillian Browne and Trudy Ramlall for technical assistance.

SUPPORTING INFORMATION AVAILABLE

Figure comparing the proteolytic digestions of SDS micelle-bound wild type and mutant αS and a description of the dependence of the fraction of free αS on the total αS concentration, the total lipid vesicle concentration, and the αS lipid vesicle affinity. This material is available free of charge via the Internet at http://pubs.acs.org.

REFERENCES

1. Polymeropoulos, M. H., Lavedan, C., Leroy, E., Ide, S. E., Dehejia, A., Dutra, A., Pike, B., Root, H., Rubenstein, J., Boyer, R., Stenroos, E. S., Chandrasekharappa, S., Athanassiadou, A., Papapetropoulos, T., Johnson, W. G., Lazzarini, A. M., Duvoisin, R. C., Di Iorio, G., Golbe, L. I., and Nussbaum, R. L. (1997) Mutation in the alpha-synuclein gene identified in families with Parkinson's disease. *Science 276*, 2045−2047.
2. Kruger, R., Kuhn, W., Muller, T., Woitalla, D., Graeber, M., Kosel, S., Przuntek, H., Epplen, J. T., Schols, L., and Riess, O. (1998) Ala30Pro mutation in the gene encoding alpha-synuclein in Parkinson's disease. *Nat. Genet. 18*, 106−108.
3. Spillantini, M. G., Schmidt, M. L., Lee, V. M., Trojanowski, J. Q., Jakes, R., and Goedert, M. (1997) Alpha-synuclein in Lewy bodies. *Nature 388*, 839−840.
4. Conway, K. A., Harper, J. D., and Lansbury, P. T. (1998) Accelerated in vitro fibril formation by a mutant alpha-synuclein linked to early-onset Parkinson disease. *Nat. Med. 4*, 1318−1320.

5. Narhi, L., Wood, S. J., Steavenson, S., Jiang, Y., Wu, G. M., Anafi, D., Kaufman, S. A., Martin, F., Sitney, K., Denis, P., Louis, J. C., Wypych, J., Biere, A. L., and Citron, M. (1999) Both familial Parkinson's disease mutations accelerate alpha-synuclein aggregation. *J. Biol. Chem. 274*, 9843−9846.
6. Conway, K. A., Lee, S. J., Rochet, J. C., Ding, T. T., Williamson, R. E., and Lansbury, P. T., Jr. (2000) Acceleration of oligomerization, not fibrillization, is a shared property of both alpha-synuclein mutations linked to early-onset Parkinson's disease: implications for pathogenesis and therapy. *Proc. Natl. Acad. Sci. U.S.A. 97*, 571−576.
7. Volles, M. J., Lee, S. J., Rochet, J. C., Shtilerman, M. D., Ding, T. T., Kessler, J. C., and Lansbury, P. T., Jr. (2001) Vesicle permeabilization by protofibrillar alpha-synuclein: implications for the pathogenesis and treatment of Parkinson's disease. *Biochemistry 40*, 7812−7819.
8. Conway, K. A., Rochet, J. C., Bieganski, R. M., and Lansbury, P. T., Jr. (2001) Kinetic stabilization of the alpha-synuclein protofibril by a dopamine-alpha-synuclein adduct. *Science 294*, 1346−1349.
9. Masliah, E., Rockenstein, E., Veinbergs, I., Mallory, M., Hashimoto, M., Takeda, A., Sagara, Y., Sisk, A., and Mucke, L. (2000) Dopaminergic loss and inclusion body formation in alpha-synuclein mice: implications for neurodegenerative disorders. *Science 287*, 1265−1269.
10. Feany, M. B., and Bender, W. W. (2000) A Drosophila model of Parkinson's disease. *Nature 404*, 394−398.
11. Clayton, D. F., and George, J. M. (1998) The synucleins: a family of proteins involved in synaptic function, plasticity, neurodegeneration and disease. *Trends Neurosci. 21*, 249−254.
12. George, J. M., Jin, H., Woods, W. S., and Clayton, D. F. (1995) Characterization of a novel protein regulated during the critical period for song learning in the zebra finch. *Neuron 15*, 361−372.
13. Weinreb, P. H., Zhen, W., Poon, A. W., Conway, K. A., and Lansbury, P. T., Jr. (1996) NACP, a protein implicated in Alzheimer's disease and learning, is natively unfolded. *Biochemistry 35*, 13709−13715.
14. Eliezer, D., Kutluay, E., Bussell, R., Jr., and Browne, G. (2001) Conformational properties of alpha-synuclein in its free and lipid-associated states. *J. Mol. Biol. 307*, 1061−1073.
15. Jensen, P. H., Hager, H., Nielsen, M. S., Hojrup, P., Gliemann, J., and Jakes, R. (1999) alpha-synuclein binds to Tau and stimulates the protein kinase A- catalyzed tau phosphorylation of serine residues 262 and 356. *J. Biol. Chem. 274*, 25481−25489.
16. Payton, J. E., Perrin, R. J., Clayton, D. F., and George, J. M. (2001) Protein−protein interactions of alpha-synuclein in brain homogenates and transfected cells. *Brain Res. Mol. Brain Res. 95*, 138−145.
17. Jenco, J. M., Rawlingson, A., Daniels, B., and Morris, A. J. (1998) Regulation of phospholipase D2: selective inhibition of mammalian phospholipase D isoenzymes by alpha- and beta-synucleins. *Biochemistry 37*, 4901−4909.
18. Davidson, W. S., Jonas, A., Clayton, D. F., and George, J. M. (1998) Stabilization of alpha-synuclein secondary structure upon binding to synthetic membranes. *J. Biol. Chem. 273*, 9443−9449.
19. Clayton, D. F., and George, J. M. (1999) Synucleins in synaptic plasticity and neurodegenerative disorders. *J. Neurosci. Res. 58*, 120−129.
20. Abeliovich, A., Schmitz, Y., Farinas, I., Choi-Lundberg, D., Ho, W. H., Castillo, P. E., Shinsky, N., Verdugo, J. M., Armanini, M., Ryan, A., Hynes, M., Phillips, H., Sulzer, D., and Rosenthal, A. (2000) Mice lacking alpha-synuclein display functional deficits in the nigrostriatal dopamine system. *Neuron 25*, 239−252.
21. Cabin, D. E., Shimazu, K., Murphy, D., Cole, N. B., Gottschalk, W., McIlwain, K. L., Orrison, B., Chen, A., Ellis, C. E., Paylor, R., Lu, B., and Nussbaum, R. L. (2002) Synaptic vesicle depletion correlates with attenuated synaptic responses to prolonged repetitive stimulation in mice lacking alpha-synuclein. *J. Neurosci. 22*, 8797−8807.
22. Schluter, O. M., Fornai, F., Alessandri, M. G., Takamori, S., Geppert, M., Jahn, R., and Sudhof, T. C. (2003) Role of alpha-synuclein in 1-methyl-4-phenyl-1,2,3,6-tetrahydropyridine-induced parkinsonism in mice. *Neuroscience 118*, 985−1002.
23. Lee, F. J., Liu, F., Pristupa, Z. B., and Niznik, H. B. (2001) Direct binding and functional coupling of alpha-synuclein to the dopamine transporters accelerate dopamine-induced apoptosis. *FASEB J. 15*, 916−926.
24. Wersinger, C., and Sidhu, A. (2003) Attenuation of dopamine transporter activity by alpha-synuclein. *Neurosci. Lett. 340*, 189−192.
25. Perrin, R. J., Woods, W. S., Clayton, D. F., and George, J. M. (2000) Interaction of human alpha-Synuclein and Parkinson's disease variants with phospholipids. Structural analysis using site-directed mutagenesis. *J. Biol. Chem. 275*, 34393−34398.
26. Jo, E., Fuller, N., Rand, R. P., St George-Hyslop, P., and Fraser, P. E. (2002) Defective membrane interactions of familial Parkinson's disease mutant A30P alpha-synuclein. *J. Mol. Biol. 315*, 799−807.
27. Cole, N. B., Murphy, D. D., Grider, T., Rueter, S., Brasaemle, D., and Nussbaum, R. L. (2002) Lipid droplet binding and oligomerization properties of the Parkinson's disease protein alpha-synuclein. *J. Biol. Chem. 277*, 6344−6352.
28. Jensen, P. H., Nielsen, M. S., Jakes, R., Dotti, C. G., and Goedert, M. (1998) Binding of alpha-synuclein to brain vesicles is abolished by familial Parkinson's disease mutation. *J. Biol. Chem. 273*, 26292−26294.
29. Bussell, R., Jr., and Eliezer, D. (2001) Residual structure and dynamics in Parkinson's disease-associated mutants of alpha-synuclein. *J. Biol. Chem. 276*, 45996−46003.
30. Bussell, R., Jr., and Eliezer, D. (2003) A structural and functional role for 11-mer repeats in alpha-synuclein and other exchangeable lipid binding proteins. *J. Mol. Biol. 329*, 763−778.
31. Freund, S. M., Wong, K. B., and Fersht, A. R. (1996) Initiation sites of protein folding by NMR analysis. *Proc. Natl. Acad. Sci. U.S.A. 93*, 10600−10603.
32. Sharon, R., Bar-Joseph, I., Frosch, M. P., Walsh, D. M., Hamilton, J. A., and Selkoe, D. J. (2003) The formation of highly soluble oligomers of alpha-synuclein is regulated by fatty acids and enhanced in Parkinson's disease. *Neuron 37*, 583−595.
33. Perrin, R. J., Woods, W. S., Clayton, D. F., and George, J. M. (2001) Exposure to long chain polyunsaturated fatty acids triggers rapid multimerization of synucleins. *J. Biol. Chem. 276*, 41958−41962.
34. El-Agnaf, O. M., Jakes, R., Curran, M. D., and Wallace, A. (1998) Effects of the mutations Ala30 to Pro and Ala53 to Thr on the physical and morphological properties of alpha-synuclein protein implicated in Parkinson's disease. *FEBS Lett. 440*, 67−70.
35. Giasson, B. I., Uryu, K., Trojanowski, J. Q., and Lee, V. M. (1999) Mutant and wild-type human alpha-synucleins assemble into elongated filaments with distinct morphologies in vitro. *J. Biol. Chem. 274*, 7619−7622.
36. Volles, M. J., and Lansbury, P. T., Jr. (2003) Zeroing in on the pathogenic form of alpha-synuclein and its mechanism of neurotoxicity in Parkinson's disease. *Biochemistry 42*, 7871−7878.
37. McLean, P. J., Kawamata, H., Ribich, S., and Hyman, B. T. (2000) Membrane association and protein conformation of alpha-synuclein in intact neurons. Effect of Parkinson's disease-linked mutations. *J. Biol. Chem. 275*, 8812−8816.
38. Kahle, P. J., Neumann, M., Ozmen, L., Muller, V., Jacobsen, H., Schindzielorz, A., Okochi, M., Leimer, U., van Der Putten, H., Probst, A., Kremmer, E., Kretzschmar, H. A., and Haass, C. (2000) Subcellular localization of wild-type and Parkinson's disease-associated mutant alpha-synuclein in human and transgenic mouse brain. *J. Neurosci. 20*, 6365−6373.
39. Chou, P. Y., and Fasman, G. D. (1978) Empirical predictions of protein conformation. *Annu. Rev. Biochem. 47*, 251−276.
40. Borhani, D. W., Rogers, D. P., Engler, J. A., and Brouillette, C. G. (1997) Crystal structure of truncated human apolipoprotein A-I suggests a lipid-bound conformation. *Proc. Natl. Acad. Sci. U.S.A. 94*, 12291−12296.
41. Eliezer, D., and Wright, P. E. (1996) Is apomyoglobin a molten globule? Structural characterization by NMR. *J. Mol. Biol. 263*, 531−538.
42. Segrest, J. P., Jones, M. K., Klon, A. E., Sheldahl, C. J., Hellinger, M., De Loof, H., and Harvey, S. C. (1999) A detailed molecular belt model for apolipoprotein A-I in discoidal high-density lipoprotein. *J. Biol. Chem. 274*, 31755−31758.
43. Spera, S., and Bax, A. (1991) Empirical correlation between protein backbone conformation and Cα and Cβ nuclear magnetic resonance chemical shifts. *J. Am. Chem. Soc. 113*, 5490−5492.
44. Wishart, D. S., Sykes, B. D., and Richards, F. M. (1991) Relationship between nuclear magnetic resonance chemical shift and protein secondary structure. *J. Mol. Biol. 222*, 311−333.

BI036135+